Songklanakarin J. Sci. Technol.
38 (4), 399-406, Jul. - Aug. 2016

http://www.sjst.psu.ac.th

Original Article

Inhibition of capsaicin and dihydrocapsaicin derivatives towards histone deacetylase and molecular docking studies

Pakit Kumboonma[1], Thanaset Senawong[3] , Khatcharin Siriwong[2], Chavi Yenjai[1], and Chanokbhorn Phaosiri[1]*

[1] *Natural Products Research Unit, Center for Innovation in Chemistry,*

[2] *Materials Chemistry Research Center, Department of Chemistry,*

[3] *Natural Products Research Unit, Department of Biochemistry, Faculty of Science, Khon Kaen University, Mueang, Khon Kaen, 40002 Thailand.*

Received: 18 September 2015; Accepted: 27 December 2015

Abstract

The natural products, capsaicin and dihydrocapsaicin, were modified at double-bond and phenolic moieties to provide twelve capsaicin and dihydrocapsaicin derivatives. The natural products and synthesized compounds were evaluated as histone deacetylase inhibitors via *in vitro* fluorometric assay at 500 mM concentrations. The results revealed that a methyl ester derivative and a silyl-protected dihydrocapsaicin were the best histone deacetylase inhibitors among the tested compounds with 87% and 85% inhibitions, respectively. Molecular docking experiments were conducted on the obtained compounds with the human HDAC8 enzyme. These data show a new method for providing putative histone deacetylase inhibitors from common natural products.

Keywords: red chili pepper, *Capsicum annuum*, histone deacetylase, HeLa cell, anticancer

1. Introduction

Anti-cancer drugs have become an essential part of global health care. Although various anti-cancer chemotherapies are widely used, an urgent need for novel anti-cancer agents remains. Plants have played a dominant role in providing herbal drugs for the treatment of a broad spectrum of diseases (Cragg *et al.,* 2009). As a part of our ongoing research program aimed at the evaluation and structural modification of bioactive secondary metabolites from plants grown widely in Thailand, we have focused our research on the phytochemicals from *Capsicum annuum*. Red chili spur pepper (*C. annuum*), or hot pepper, is regularly used as a spice in Thai cuisine. Several experiments have been conducted to explore the clinical applications of natural products from this plant species (Laohavechvanich *et al.,* 2006; Hayman *et al.,* 2008). Capsaicin and dihydrocapsaicin, the spicy agents in chili peppers, partially mimic the structure of the FDA-approved histone deacetylase (HDAC) inhibitors suberoylanilide hydroxamic acid (**1**, SAHA, Vorinostat®, Zolinza™ (Paris *et al*., 2008) and trichostatin A (**2**, TSA). Therefore, capsaicin derivatives may also inhibit histone deacetylase. SAHA is approved for the treatment of a rare cancer, cutaneous T-cell lymphoma, in patients who have progressive, persistent or recurrent disease.

Histone deacetylase inhibitors can affect differentiation, growth arrest, or apoptosis in transformed cell cultures by blocking substrate access to the histone deacetylase-active site (Bertrand *et al.,* 2010). The results obtained from X-ray crystallography and the structure–activity relation-

* Corresponding author.
Email address: chapha@kku.ac.th

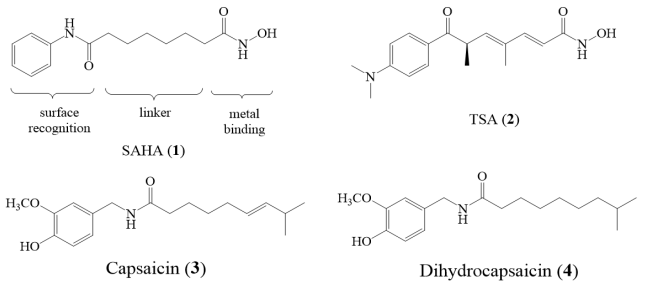

Figure 1. The pharmacophoric summary of HDAC inhibitor structural characteristics in comparison to the structures of capsaicin and dihydrocapsaicin.

ships of SAHA have provided the structural characteristics of HDAC inhibitors, as depicted in Figure 1 (Finnin *et al.,* 1999). The pharmacophore of HDAC inhibitors is composed of a metal-binding domain, a linker domain, and a surface-recognition domain. The metal-binding functional group is responsible for binding a Zn^{2+} ion in the active site of the HDAC enzyme, whereas the hydrocarbon linker domain plays a role in filling out a narrow tunnel leading to the active site. Finally, the capping group on the surface-recognition domain interacts with the amino acids close to the entrance to the HDAC active site. A structural comparison between SAHA, TSA and capsaicin, as shown in Figure 1, guided possible modifications of capsaicin to improve HDAC inhibitory activity. For example, the polar phenolic group of capsaicin should be converted into a less-polar moiety to increase surface recognition. Moreover, the hydrophobic double-bond side chain of capsaicin may be installed to provide a compound with a better metal-binding affinity.

In this work, we evaluate capsaicin (CAP), dihydrocapsaicin (DHC) as well as structural modifications of these lead compounds, as an HDAC inhibitor to explore the potential inhibitory activity of capsaicin and dihydrocapsaicin derivatives. These derivatives exhibit promising HDAC inhibition and may warrant further studies at the cellular level.

2. Materials and Methods

2.1 Plant material

Dried red chili spur peppers (*Capsicum annuum*) were purchased from the local market in Khon Kaen Province, Thailand. One kilogram of plant materials was extracted as previously described to provide a mixture of Capsaicin (CAP, **3**) and Dihydrocapsaicin (DHC, **4**) (690 mg) as a yellow-orange oil (Kumboonma *et al.,* 2009).

2.2 Structural modifications

Structural modifications of a CAP/DHC mixture were performed without further purification to obtain various derivatives as demonstrated in Scheme 1 and Figure 2 (Kumboonma *et al.,* 2010). All compounds were characterized by using spectroscopy techniques including IR, NMR and MS.

N-(4-hydroxy-3-methoxybenzyl)-5-(3-isopropyloxiran-2-yl) pentanamide (**5**)

R_f 0.30 (1:1 EtOAc/hexane). IR (neat) 3333, 2932, 1741, 1645, 1515, 1463, 1372, 1277, 1125, 1036 cm^{-1}. ^1H NMR (400 MHz, $CDCl_3$) δ 6.84 (d, J = 8.4 Hz, $1H_5$), 6.80 (s, $1H_2$), 6.72 (d, J = 8.4 Hz, $1H_6$), 5.86 (br s, OH), 5.85 (s, $1H_8$), 4.35 (d, J = 5.4 Hz, $2H_7$), δ 3.85 (s, OCH_3), 2.70 (m, $1H_{14}$), 2.42 (dd, J = 2.2, 7.0 Hz, $1H_{15}$), 2.20 (t, J = 7.6 Hz, $2H_{10}$), 1.70 (m, $2H_{11}$), 1.52 (m, $1H_{16}$), 1.50 (m, $2H_{13}$), 1.45 (m, $2H_{12}$), 0.95 (d, J = 6.6 Hz, $3H_{17}$), 0.90 (d, J = 6.6 Hz, $3H_{18}$). ^{13}C NMR (100 MHz, $CDCl_3$) δ 172.69 (C_9), 146.75 (C_3), 145.13 (C_4), 130.20 (C_1), 120.73 (C_6), 114.44 (C_5), 110.77 (C_2), 64.24 (C_{15}), 57.61 (C_{14}), 55.91 (OCH_3), 43.53 (C_7), 36.46 (C_{10}), 31.74 (C_{13}), 30.47 (C_{12}), 25.74 (C_{16}), 25.41 (C_{11}), 19.00 (C_{17}), 18.37 (C_{18}). HRMS-ESI (*m/z*) $[M + Na]^+$ calcd for $C_{18}H_{27}NO_4$ + Na 344.1838, found 344.1840.

6-Hydroxy-*N*-(4-hydroxy-3-methoxybenzyl)-8-methylnonanamide (**6**)

R_f 0.20 (1:1 EtOAc/hexane). IR (neat) 3334, 2933, 2867, 1715, 1645, 1515, 1274, 1035, 820, 741 cm^{-1}. ^1H NMR (400 MHz, $CDCl_3$) δ 6.86 (d, J = 8.0 Hz, $1H_5$), 6.80 (s, $1H_2$), 6.75 (d, J = 8.0 Hz, $1H_6$), 5.70 (br s, $1H_8$), 5.65 (br s, OH_4), 4.35 (d, J = 5.4 Hz, $2H_7$), 3.85 (s, OCH_3), 3.65 (m, $1H_{14}$), 2.20 (t, J = 7.8 Hz, $2H_{10}$), 1.70 (m, $2H_{11}$), 1.62 (m, $1H_{16}$), 1.50 (m, $2H_{13}$), 1.45 (m, $2H_{12}$), 1.40 (m, $1H_{15}$), 0.90 (d, J = 6.6 Hz, $3H_{17}$), 0.90 (d, J = 6.6 Hz, $3H_{18}$). ^{13}C NMR (100 MHz, $CDCl_3$) δ 172.82 (C_9), 146.68 (C_3), 145.12 (C_4), 130.26 (C_1), 120.81 (C_6), 114.37 (C_5), 110.73 (C_2), 69.62 (C_{14}), 55.94 (OCH_3), 46.84 (C_{15}), 43.57 (C_7), 37.50 (C_{13}), 36.58 (C_{10}), 25.53 (C_{11}), 25.19 (C_{12}), 24.60 (C_{16}), 23.44 (C_{17}), 22.04 (C_{18}). HRMS-ESI (*m/z*) $[M + Na]^+$ calcd for $C_{18}H_{29}NO_4$ + Na 346.1994, found 346.1999.

(*E*)-9-(4-acetoxy-3-methoxybenzylamino)-2-methyl-9-oxonon-3-en-5-yl acetate (**7**)

R_f 0.60 (1:1 EtOAc/hexane). IR (neat) 3295, 3071, 2956, 2869, 1768, 1731, 1646, 1514, 1464, 1422, 1372, 1247, 1153, 1020 cm^{-1}. ^1H NMR (400 MHz, $CDCl_3$) δ 6.98 (d, J = 8.0 Hz, $1H_5$), 6.90 (s, $1H_2$), 6.85 (d, J = 8.0 Hz, $1H_6$), 5.80 (s, $1H_8$), 4.95 (m, $1H_{14}$), 4.40 (d, J = 5.7 Hz, $2H_7$), 3.80 (s, OCH_3), 2.30 (s, $3H_{20}$), 2.20 (t, J = 7.8 Hz, $2H_{10}$), 2.00 (s, $3H_{22}$), 1.65 (m, $2H_{11}$), 1.52 (m, $2H_{13}$), 1.50 (m, $1H_{15}$), 1.30 (m, $2H_{12}$), 1.26 (m, $1H_{16}$), 0.90 (d, J = 6.2 Hz, $3H_{17}$), 0.90 (d, J = 6.2 Hz, $3H_{18}$). ^{13}C NMR (100 MHz, $CDCl_3$) δ 172.59 (C_9), 170.94 (C_{21}), 169.10 (C_{19}), 151.19 (C_3), 139.07 (C_4), 137.32 (C_1), 122.85 (C_5), 120.01 (C_6), 112.19 (C_2),

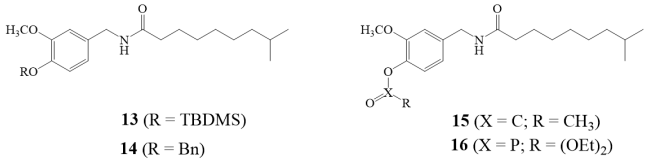

Figure 2. Structures of synthetic dihydrocapsaicin derivatives.

72.39 (C_{14}), 55.89 (OCH_3), 43.45 (C_7), 43.33 (C_{15}), 36.53 (C_{10}), 34.47 (C_{13}), 25.50 (C_{11}), 24.93 (C_{12}), 24.65 (C_{16}), 23.13 (C_{17}), 22.16 (C_{18}), 21.24 (C_{22}), 20.62 (C_{20}). HRMS-ESI (*m/z*) $[M + Na]^+$ calcd for $C_{22}H_{33}NO_6$ + Na 430.2206, found 430.2209.

N-(4-(*tert*-butyldimethylsilyloxy)-3-methoxybenzyl)-6, 7-dihydroxy-8-methylnonanamide (**8**)

R_f 0.15 (1:1 EtOAc/hexanes). IR (neat) 3306, 2930, 2857, 1714, 1634, 1514, 1463, 1283, 1254, 1159, 1127, 1037, 901, 840, 783 cm^{-1}. ^1H NMR (400MHz, $CDCl_3$) δ 6.78 (d, J = 8.0 Hz, $1H_5$), 6.76 (s, $1H_2$), 6.70 (d, J = 8.0 Hz, $1H_6$), 5.85 (br s, $1H_8$), 4.25 (d, J = 5.3 Hz, $2H_7$), 3.78 (s, OCH_3), 3.60 (q, J = 4.7 Hz, $1H_{14}$), 3.15 (t, J = 5.1 Hz, $1H_{15}$), 2.25 (m, $2H_{10}$), 2.25 (m, $2H_{13}$), 2.25 (m, $1H_{16}$), 1.78 (m, $2H_{11}$), 1.50 (m, $2H_{12}$), 0.98 (s, $9H_{21}$), 0.94 (d, J = 6.6 Hz, $3H_{18}$), 0.92 (d, J = 6.6 Hz, $3H_{17}$), 0.15 (s, $6H_{19}$). ^{13}C NMR (100 MHz, $CDCl_3$) δ 172.92 (C_9), 151.07 (C_3), 144.53 (C_4), 131.62 (C_1), 120.87 (C_6), 120.20 (C_5), 112.04 (C_2), 78.99 (C_{15}), 71.47 (C_{14}), 55.54 (OCH_3), 43.57 (C_7), 36.46 (C_{10}), 33.41 (C_{13}), 30.13 (C_{12}), 25.68 (C_{11}), 25.37 (C_{20}), 25.15 (C_{16}), 19.73 (C_{18}), 18.42 (C_{17}), 17.02 (C_{21}), -4.66 (C_{19}). HRMS-ESI (*m/z*) $[M + H]^+$ calcd for $C_{24}H_{44}NO_5Si^+$ 454.2989, found 454.3000.

N-(4-(*tert*-butyldimethylsilyloxy)-3-methoxybenzyl)-6-oxohexanamide (**9**)

R_f 0.50 (1:1 EtOAc/hexanes). IR (neat) 3296, 3071, 2929, 2857, 2719, 1723, 1645, 1514, 1463, 1419, 1284, 1254, 1159, 1127, 1037, 902, 840, 783 cm^{-1}. ^1H NMR (400 MHz, $CDCl_3$) δ 9.75 (s, $1H_{14}$), 6.78 (d, J = 7.9 Hz, $1H_5$), 6.76 (s, $1H_2$), 6.70 (d, J = 7.9 Hz, $1H_6$), 5.78 (br s, $1H_8$), 4.35 (d, J = 5.5 Hz, $2H_7$), 3.78 (s, OCH_3), 2.35 (t, J = 6.1 Hz, $2H_{13}$), 2.10 (t, J = 6.8 Hz, $2H_{10}$), 1.70 (m, $2H_{12}$), 1.70 (m, $2H_{11}$), 0.98 (s, $9H_{21}$), 0.15 (s, $6H_{19}$). ^{13}C NMR (100MHz, $CDCl_3$) δ 202.15 (C_{14}), 172.12 (C_9), 151.06 (C_3), 144.52 (C_4), 131.60 (C_1), 120.86 (C_6), 120.19 (C_5), 111.98 (C_2), 55.48 (OCH_3), 43.56 (C_7), 43.55 (C_{13}), 36.28 (C_{10}), 25.68 (C_{16}), 25.04 (C_{11}), 21.54 (C_{17}), 18.41 (C_{12}), -4.67 (C_{15}).

HRMS-ESI (*m/z*) $[M + H]^+$ calcd for $C_{20}H_{34}NO_4Si^+$ 380.2257, found 380.2257. 6, 7-Dihydroxy-*N*-(4-hydroxy-3-methoxybenzyl)-8-methylnonanamide (**10**)

R_f 0.15 (EtOAc). IR (neat) 3435, 1634, 667 cm^{-1}. ^1H NMR (400MHz, $CDCl_3$) δ 6.85 (d, J = 8.0 Hz, $1H_5$), 6.80 (s, $1H_2$), 6.75 (d, J = 8.0 Hz, $1H_6$), 5.85 (br s, $1H_8$), 4.62 (s, OH_{14}), 4.62 (s, OH_{15}), 4.35 (d, J = 5.3 Hz, $2H_7$), 3.85 (s, OCH_3), 3.58 (q, J = 4.7 Hz, $1H_{14}$), 3.10 (t, J = 5.1 Hz, $1H_{15}$), 2.20 (m, $2H_{10}$), 2.20 (m, $2H_{13}$), 1.85 (m, $1H_{16}$), 1.70 (m, $2H_{11}$), 1.50 (m, $2H_{12}$), 0.94 (d, J = 6.6 Hz, $3H_{18}$), 0.92 (d, J = 6.6 Hz, $3H_{17}$). ^{13}C NMR (100 MHz, $CDCl_3$) δ 172.91 (C_9), 146.71 (C_3), 145.10 (C_4), 130.23 (C_1), 120.78 (C_6), 114.43 (C_5), 110.76 (C_2), 78.97 (C_{14}), 71.47 (C_{15}), 55.95 (OCH_3), 43.54 (C_7), 36.41 (C_{10}), 33.36 (C_{13}), 30.09 (C_{12}), 25.33 (C_{11}), 25.11 (C_{16}), 19.71 (C_{18}), 16.96 (C_{17}).

HRMS-ESI (*m/z*) $[M + H]^+$ calcd for $C_{18}H_{30}NO_5^+$ 340.2124, found 340.2010. Methyl-6-(2-bromo-4-(*tert*-butyldimethyl-silyloxy)-5-methoxybenzylamino)-6-oxohexanoate (**11**)

R_f 0.60 (1:1 EtOAc/hexanes). IR (neat) 3296, 3289, 3074, 2953, 2932, 2857, 1738, 1651, 1504, 1257, 1205, 1040, 969, 904, 840, 784 cm^{-1}. ^1H NMR (400MHz, $CDCl_3$) δ 7.00 (s, $1H_5$), 6.88 (s, $1H_2$), 5.95 (br s, $1H_8$), 4.40 (d, J = 5.9 Hz, $2H_7$), 3.78 (s, OCH_3), 3.62 (s, $3H_{15}$), 2.35 (t, J = 7.0 Hz, $2H_{13}$), 2.20 (t, J = 7.0 Hz, $2H_{10}$), 1.65 (m, $2H_{11}$) 1.65 (m, $2H_{12}$), 0.98 (s, $9H_{18}$), 0.15 (s, $6H_{16}$). ^{13}C NMR (100 MHz, $CDCl_3$) δ 173.82 (C_{14}), 172.32 (C_9), 150.50 (C_3), 145.29 (C_4), 130.29 (C_1), 124.59 (C_5), 114.10 (C_6), 113.42 (C_2), 55.62 (OCH_3), 51.51 (C_{15}), 43.65 (C_7), 36.17 (C_{10}), 33.64 (C_{13}), 25.60 (C_{17}), 25.03 (C_{11}), 24.39 (C_{12}), 18.39 (C_{18}), -4.69 (C_{16}). HRMS-ESI (*m/z*) $[M + H]^+$ calcd for $C_{21}H_{35}NO_5SiBr^+$ 488.1468, found 488.1468.

Methyl-6-(2-bromo-4-hydroxy-5-methoxybenzylamino)-6-oxohexanoate (**12**)

R_f 0.35 (1:1 EtOAc/hexanes). IR (neat) 3360, 2951, 1642, 1505, 1275, 1202, 1036 cm^{-1}. ^1H NMR (400MHz, $CDCl_3$) δ 7.08 (s, $1H_5$), 6.92 (s, $1H_2$), 6.00 (br s, $1H_8$), 4.40 (d, J = 6.0 Hz, $2H_7$), 3.85 (s, OCH_3), 3.65 (s, $3H_{15}$), 2.35 (t, J = 6.9 Hz, $2H_{13}$), 2.20 (t, J = 6.9 Hz, $2H_{10}$), 1.65 (m, $2H_{11}$) 1.65 (m, $2H_{12}$). ^{13}C NMR (100 MHz, $CDCl_3$) δ 173.85 (C_{14}), 172.42 (C_9), 146.09 (C_3), 145.92 (C_4), 128.83 (C_1), 118.44 (C_5), 114.40 (C_6), 113.15 (C_2), 56.15 (OCH_3), 51.53 (C_{15}), 43.70 (C_7), 36.17 (C_{10}), 33.64 (C_{13}), 25.00 (C_{11}), 24.38 (C_{12}). HRMS-ESI (*m/z*) $[M + H]^+$ calcd for $C_{15}H_{21}NO_5Br^+$ 374.0603, found 374.0603.

N-(4-(*tert*-butyl-dimethylsilyloxy)-3-methoxybenzyl)-8-methylnonanamide (**13**)

R_f 0.85 (1:1 EtOAc/hexanes). IR (neat) 3290, 2923, 1645, 1515, 1286, 1159, 1126, 1036, 902, 840 cm^{-1}. ^1H NMR (400 MHz, $CDCl_3$) δ 6.79 (d, J = 8.4 Hz, $1H_5$), 6.75 (s, $1H_2$), 6.70 (d, J = 8.4 Hz, $1H_6$), 5.70 (br s, $1H_8$), 4.38 (d, J = 5.4 Hz, $2H_7$), 3.79 (s, OCH_3), 2.20 (t, J = 7.8 Hz, $2H_{10}$), 1.98 (q, J = 7.2 Hz, $2H_{13}$), 1.64 (quin, J = 7.8 Hz, $2H_{11}$), 1.40 (quin, J = 7.8 Hz, $2H_{12}$), 1.29 (m, $1H_{16}$), 1.26 (m, $2H_{14}$), 1.13 (m, $2H_{15}$), 1.00 (s, $9H_{21}$), 0.95 (d, J = 6.6 Hz, $3H_{17}$), 0.95 (d, J = 6.6 Hz, $3H_{18}$), 0.18 (s, $6H_{19}$). ^{13}C NMR (100 MHz, $CDCl_3$) δ 172.52 (C_9), 150.62 (C_3), 144.03 (C_4), 131.31 (C_1), 120.38 (C_6), 119.68 (C_5), 111.48 (C_2), 55.01 (OCH_3), 43.03 (C_7), 38.92 (C_{15}), 36.21 (C_{10}), 31.75 (C_{16}), 29.16 (C_{13}), 28.81 (C_{12}), 27.21 (C_{14}), 25.37 (C_{21}), 24.84 (C_{11}), 22.18 (C_{17}), 22.18 (C_{18}), 17.97 (C_{20}), -5.11 (C_{19}). HRMS-ESI (*m/z*) $[M + Na]^+$ calcd for $C_{24}H_{43}NO_3Si$ + Na 444.2910, found 444.2913.

N-(4-(benzyloxy)-3-methoxybenzyl)-8-methylnonanamide (**14**)

R_f 0.75 (1:1 EtOAc/hexanes). IR (neat) 3317, 2930, 2863, 1636, 1542, 1465, 1456, 1256, 1235, 1137, 1030, 1010 cm^{-1}. ^1H NMR (400 MHz, $CDCl_3$) δ 7.42 (d, J = 8.4 Hz, $2H_{22}$), 7.28 (t, J = 8.4 Hz, $2H_{23}$), 7.25 (d, J = 8.4 Hz, $2H_{21}$), 6.84 (s, $1H_2$), 6.82 (d, J = 8.4 Hz, $1H_5$), 6.75 (d, J = 8.4 Hz, $1H_6$), 6.65 (s, $1H_8$), 5.15 (s, $2H_{19}$), 4.38 (d, J = 5.4 Hz, $2H_7$), 3.79 (s, OCH_3), 2.20 (t, J = 7.8 Hz, $2H_{10}$), 1.98 (q, J = 7.2 Hz, $2H_{13}$), 1.65 (m, $2H_{11}$), 1.40 (m, $2H_{12}$), 1.29 (m, $1H_{16}$), 1.26 (m, $2H_{14}$), 1.13 (m, $2H_{15}$), 0.95 (d, J = 6.6 Hz, $3H_{17}$), 0.95 (d, J = 6.6 Hz, $3H_{18}$). ^{13}C NMR (100 MHz, $CDCl_3$) δ 172.80 (C_9), 149.87 (C_3), 147.58 (C_4), 137.07 (C_{20}), 131.57 (C_1), 128.51 (C_{22}), 127.82 (C_{23}), 127.21 (C_{21}), 120.01 (C_6), 114.10 (C_5), 111.76 (C_2), 71.10 (C_{19}), 56.00 (OCH_3), 43.42 (C_7), 38.92 (C_{15}), 36.67 (C_{10}), 32.19 (C_{16}), 29.59 (C_{13}), 29.34 (C_{12}), 27.21 (C14), 25.25 (C_{11}), 22.63 (C_{17}), 22.63 (C_{18}). HRMS-ESI

(*m/z*) $[M + Na]^+$ calcd for $C_{25}H_{35}NO_3$ + Na 420.2515, found 420.2518.

2-Methoxy-4-((8-methylnonanamido)methyl) phenylacetate (**15**)

R_f 0.70 (1:1 EtOAc/hexanes). IR (neat) 3296, 3071, 2927, 2855, 2227, 1767, 1646, 1607, 1541, 1512, 1464, 1421, 1360, 1271, 1199, 1122, 1036 cm^{-1}. ^1H NMR (400 MHz, $CDCl_3$) δ 6.95 (d, J = 8.4 Hz, $1H_5$), 6.88 (s, $1H_2$), 6.80 (d, J = 8.4 Hz, $1H_6$), 5.95 (s, $1H_8$), 4.35 (d, J = 5.4 Hz, $2H_7$), 3.79 (s, OCH_3), 2.28 (s, $3H_{20}$), 2.20 (t, J = 7.8 Hz, $2H_{10}$), 1.98 (q, J = 7.2 Hz, $2H_{13}$), 1.64 (m, $2H_{11}$), 1.40 (m, $2H_{12}$), 1.29 (m, $1H_{16}$), 1.26 (m, $2H_{14}$), 1.13 (m, $2H_{15}$), 0.95 (d, J = 6.6 Hz, $3H_{17}$), 0.95 (d, J = 6.6 Hz, $3H_{18}$). ^{13}C NMR (100 MHz, $CDCl_3$) δ 173.21 (C_9), 169.12 (C_{19}), 151.15 (C_3), 139.01 (C_4), 137.37 (C_1), 122.78 (C_5), 119.95 (C_6), 112.10 (C_2), 55.85 (OCH_3), 43.38 (C_7), 38.92 (C_{15}), 36.53 (C_{10}), 32.19 (C_{16}), 29.60 (C_{13}), 29.27 (C_{12}), 27.21 (C_{14}), 25.25 (C_{11}), 22.62 (C_{17}), 22.62 (C_{18}), 20.61 (C_{20}). HRMS-ESI (*m/z*) $[M + Na]^+$ calcd for $C_{20}H_{31}NO_4$ + Na 372.2151, found 372.2151.

Diethyl-2-methoxy-4-((8methylnonanamido) methyl) phenyl phosphate (**16**)

R_f 0.45 (1:1 EtOAc/hexanes). IR (neat) 3302, 3073, 2929, 2867, 1651, 1514, 1464, 1274, 1213, 1157, 1126, 1034, 969, 820 cm^{-1}. ^1H NMR (400 MHz, $CDCl_3$) δ 7.19 (d, J = 8.4 Hz, $1H_5$), 6.85 (s, $1H_2$), 6.78 (d, J = 8.4 Hz, $1H_6$), 5.95 (s, $1H_8$), 4.35 (d, J = 5.4 Hz, $2H_7$), 4.20 (q, J = 8.0 Hz, $4H_{19}$), 3.79 (s, OCH_3), 2.20 (t, J = 7.8 Hz, $2H_{10}$), 1.98 (q, J = 7.2 Hz, $2H_{13}$), 1.64 (m, $2H_{11}$), 1.38 (m, $2H_{12}$), 1.35 (t, J = 8.0 Hz, $6H_{20}$), 1.29 (m, $1H_{16}$), 1.26 (m, $2H_{14}$), 1.13 (m, $2H_{15}$), 0.95 (d, J = 6.6 Hz, $3H_{17}$), 0.95 (d, J = 6.6 Hz, $3H_{18}$). ^{13}C NMR (100 MHz, $CDCl_3$) δ 173.08 (C_9), 150.75 (C_3), 139.16 (C_4), 136.27 (C_1), 121.28 (C_6), 119.89 (C_5), 112.38 (C_2), 64.57 (C_{19}), 55.92 (OCH_3), 43.24 (C_7), 38.92 (C_{15}), 36.49 (C_{10}), 32.19 (C_{16}), 29.59 (C_{13}), 29.26 (C_{12}), 27.21 (C_{14}), 25.25 (C_{11}), 22.59 (C_{17}), 22.59 (C_{18}), 15.99 (C_{20}). HRMS-ESI (*m/z*) $[M + Na]^+$ calcd for $C_{26}H_{38}NO_6P$ + Na 466.2334, found 466.2341.

2.3 Histone deacetylase activity assay

Capsaicin, dihydrocapsaicin and their synthetic derivatives were evaluated for their ability to inhibit a commercially available assay (Fluor de Lys assay system, Biomol, Enzo Life Sciences International, Inc., USA). TSA (**2**) purchased from Sigma-Aldrich Corporation (USA) was used as the positive control. The substrate, extract and inhibitors were incubated. Deacetylation of the substrate followed with adding the developer generated a fluorophore. Comparison of inhibitor versus control relative fluorescence signals with excitation at 360 nm and emission at 460 nm using the spectra Max Gemini XPS microplate spectrofluorometer (Molecular Devices, USA) determined percent HDAC activity remaining. All experiments were carried out in triplicate.

2.4 Molecular docking studies

Molecular docking studies were performed for 50 runs using AutoDockTools 1.5.4 (ADT) and AutoDock 4.2 programs with a grid box size of 66×66×66 points and Lamarckian genetic algorithm search (Sanner *et al.,* 1999; Morris *et al.,* 2009). The crystal structures of human histone deacetylase HDAC8 [PDB entry code: 1T64, complexed with the inhibitor, TSA, resolution: 1.90 Å] was obtained from the Protein Data Bank (available from http://www.rcsb.org, last accessed 30 November 2009). All water and non-interacting ions as well as TSA were removed. Then all missing hydrogen and sidechain atoms were added using the ADT program. Gasteiger charges were calculated for the system. For ligand setup, the molecular modeling program Hyperchem 8.0 was used to build the ligands (HyperChem Professional 8.0, HyperCube, Inc., Florida, USA, 2007). These ligands were optimized with the AM1 level.

3. Results and Discussion

Capsaicin (CAP, **3**) was isolated from *C. annuum* fruits as a mixture with dihydrocapsaicin (DHC, **4**). The separation of these two natural products was unsuccessfully attempted with different column chromatography methods. Therefore, structural modification of a CAP/DHC mixture was performed without further purification, as shown in Scheme 1. CAP (**3**) was reduced into DHC (**4**) in a good yield. The mixture of **3** and 4 was oxidized by *m*CPBA to produce the epoxide **5** along

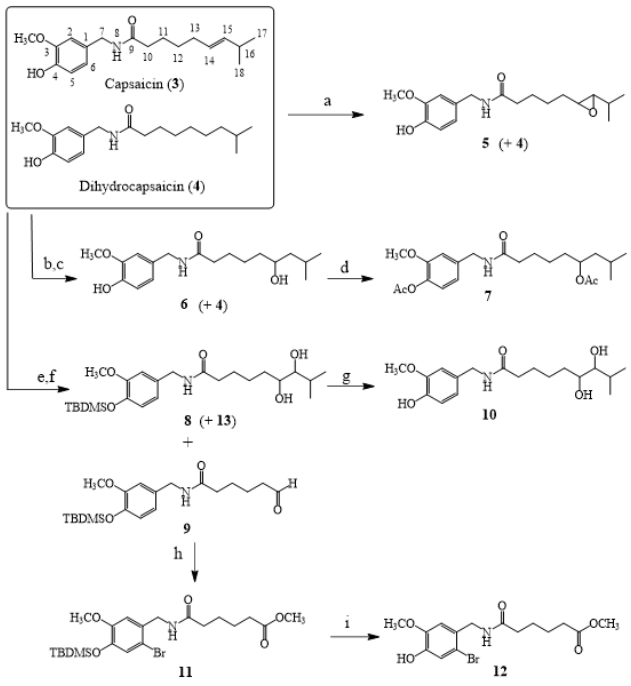

Scheme 1. Reagents and conditions: (a) *m*CPBA, EtOAc, rt, 74%; (b) $Hg(OAc)_2$, H_2O, CH_3COOH, rt; (c) $NaBH_4$, NaOH, rt, 91% (2 steps); (d) Ac_2O, Pyridine, rt, 73%; (e) NaH, TBDMSCl, THF, reflux; (f) $NaIO_4$, K_2OsO_4, H_2O, rt, 65% for **8** and 35% for **9** in 2 steps; (g) TBAF, THF, 0°C, 90%; (h) Br_2, $NaHCO_3$, MeOH, H_2O, rt, 69%; (i) TBAF, THF, 0°C, 82%.

with recovery of **4**. Formation of the alcohol **6** was achieved by treating the **3** and **4** mixture with $Hg(OAc)_2$ and followed with $NaBH_4$. The structure of **6** was confirmed by 2D NMR experiments. The correlation between C_{14} and H_{16} could be observed from the CIGAR experiment. The racemic mixture of alcohol **6** was readily converted into diacetate **7**, via reaction of **6** with acetic anhydride and pyridine. The diol **8** was obtained as a mixture of enantiomers after *syn*-dihydroxylation of the silyl protected **3** and **4** with $NaIO_4$ and K_2OsO_4. The aldehyde 9 was also gained as a minor product as well as the silyl ether derivative of DHC (**13**) which is shown in Figure 2. This oxidative cleavage condition was tried with **3** and **4**, but it led to a decomposition of starting materials. Further oxidation of the aldehyde **9** was carried out with bromine in methanol to give methyl ester **11**. Under this condition, the bromine atom replaced the hydrogen atom at the C_6 position in aromatic region of **11**. The silyl group of **11** was removed by using TBAF to give methyl ester **12** in a good yield. Reaction between the previously obtained diol **8** and TBAF also provided the racemic mixture of the dihydroxy DHC **10** in a high yield. The spectroscopic data of **10** confirmed the structure of major regioisomer **6** which was gained from oxymercuration-demercuration of **3**. The ^{1}HNMR signals of H_{14} which belonged to **6** and **10** appeared at 3.65 ppm and 3.58 ppm, respectively. The DHC synthetic derivative structures are depicted in Figure 2. The phenolic group of **4** was protected as silyl ether, benzyl ether, acetate ester and phosphate ester to provide **13**, **14**, **15** and **16**, respectively.

CAP **3**, DHC **4** and their synthetic derivatives were screened *in vitro* using a HeLa nuclear extract in a fluorometric assay at 500 μM concentrations. The inhibitory activities of all compounds against HDAC *in vitro* are presented in Table 1. Molecular docking studies were conducted with the human HDAC8 to gain more details on the binding mode and to obtain additional validation of the experimental results. All compounds were analyzed to allow comparisons of the calculated free energies of binding (ΔG) and inhibition constants (K_i), which are also shown in Table 1. The mixture of **3** and **4** showed no activity at 500 μM concentrations. Notably, compound 4 alone also exhibited no activity at the same concentration as the mixture of **3** and **4**. These results indicate that no significant difference exists between a saturated side chain and one with a single double-bond. Modification of the double-bond side chain provided the epoxide **5** with no inhibitory activity. The results suggest that electron density of the epoxide functional group may not be enough for binding to the active site of HDAC. Six compounds (**6**, **7**, **10**, **11**, **12** and **13**) showed inhibitory activities against HDAC. Although the inhibitory activities were not comparable to that of TSA, these results provide valuable information regarding active-site binding to HDAC.

The incorporation of a hydroxy group and a dihydroxy group in the alkyl chains was conducted to gain compounds **6** and **8**, which were expected to exhibit improved coordinating and chelating properties to the zinc ion. Surprisingly, only **6** showed inhibitory activity against HDAC with 80% inhibition. The HDAC inhibitory activity test of compound **7** was performed to examine whether the acetate ester in the alkyl side chain improved activity. Compound **7** exhibited 83% inhibition against HDAC. These data indicated that the hydroxy and acetyl groups can act as alternative zinc coordinating groups and provide better metal binding than the epoxide functional group. After the silyl group removal from **8**, the dihydroxycapsaicin **10** was obtained and its inhibitory activity against HDAC increased dramatically. Therefore, the silyl group of **8** may be too bulky to allow ligand-enzyme

Table 1. *In vitro* and *in silico* HDAC inhibitory activities of the obtained compounds.

Compound	HDAC Inhibitory Activities (%)	ΔG (kcal/mol)	K_i (μM)
1		-6.23	26.9
2[a]	69 ± 1.09	-6.91	8.6
3 and 4	inactive	-	-
4	inactive	-4.71	355.3
5	inactive	-4.39	610.49
6	80 ± 0.75	-5.41	108.7
7	83 ± 0.51	-5.46	99.5
8	inactive	-4.56	453.89
9	inactive	-4.54	471.73
10	75 ± 0.95	-4.93	243.67
11	55 ± 1.03	-4.89	258.68
12	87± 0.73	-5.08	198.14
13	85± 0.85	-4.99	218.17
14	inactive	-4.57	443.12
15	inactive	-4.37	630.51
16	inactive	-3.56	2470

[a] Positive control at 25 μM

binding or reinforce the dihydroxy group from chelating to the zinc ion. This hypothesis can be applied to explain the results obtained from the inactive aldehyde **9** and the slightly active methyl ester **11** against HDAC. The increasing inhibitory activity of the methyl ester **12** may be mainly due to chelating of the methyl ester functional group to the zinc ion. Interestingly, the bromine atom at C_6 of **12** did not restrict inhibitor-enzyme interaction. The biological data reported herein suggest that the highly polar functional groups play an important role in metal binding for HDAC. The HDAC inhibitory activities of compounds **13**, **14**, **15** and **16** were tested to examine whether the hydrophobic ether or ester groups of the aromatic region increased the activities. However, only modification of the hydroxyl group into *tert*-butyldimethyl silyl ether in **13** resulted in increasing activity, with 85% inhibition. Apparently, the ester moieties did not provide enough electronic interaction between the enzyme and the inhibitor. The lack of activity with the ester moieties is most likely due to the polarized p-bonds. Of the two ether protecting groups (*tert*-butyldimethyl silyl ether in compound **13** and benzyl ether in compound **14**), **13** demonstrated a better interaction with the enzyme. The *tert*-butyldimethyl silyl ether can be assumed to be of compatible size with the hydrophobic pocket of the enzyme. As is evident from the results, the hydrophobic aromatic region is critical for binding, which is in agreement with the crystal structure (Vannini *et al.,* 2004).

Molecular docking studies were conducted to gain more details on the binding mode of the synthetic derivatives and to obtain additional validation of the experimental results. Visual inspection of the binding mode for SAHA (**1**) at HDAC8 binding site showed that its hydroxamic acid group approaches the zinc ion making ionic interaction with the zinc ion (Figure 3A). HIS180, HIS142, HIS143 and TYR306 are the other residues near the cofactor zinc ion along with the hydroxamic group of the inhibitor. There are four important interactions considered as hydrogen bonds. The hydrogen bond between the hydroxy group of TYR306 and the carbonyl moiety of the hydroxamic acid group was calculated as 2.6 Å. The imidazole moiety of the HIS143 is H-bonded to the amino part of the hydroxamic acid group (3.1 Å). The other hydrogen bond is between the hydroxy group of the hydroxamic acid and the imidazole moiety of HIS142 (2.7 Å). Finally, a hydrogen bond is observed between the hydroxy group of hydroxamic group and the imidazole moiety of HIS180 (2.3 Å). The high inhibition potency of SAHA (**1**) toward HDAC8 can be justified by these four strong hydrogen bonds as shown in Table 1. These results are relevant to that of the crystal structure of human HDAC8 complexed with the hydroxamic acid inhibitor (Finnin *et al.,* 1999). Visual inspection of the position of **6** in the HDAC8 binding site shows that ASP87 and TYR100 are the residues near the aromatic and the amide regions of **6** (Figure 3B). Three important interactions are considered to be hydrogen bonds. One hydrogen bond occurs between the backbone carbonyl group of TYR100 and the hydrogen atom of the amide group that belongs to **6** (2.6 Å). Two hydrogen bonds are observed from coordinating between carboxylic group of ASP87 and the hydrogen atom at phenolic group of **6** (2.9 Å, 3.4 Å). Notably, the hydroxy group in the alkyl side chain of **6** forms a weak interaction with the zinc ion. This binding mode correlates well with the initially designed inhibitors. Moreover, a considerably lower inhibition constant is calculated for **6** compared to that of the previously mentioned capsaicin derivatives.

The major interaction between HDAC8 and compound **7** is the hydrogen bond between the hydroxy group of TYR100 and the carbonyl moiety of the acetyl group on the side chain of TYR100 (2.9 Å) as shown in Figure 4A. Surprisingly, the amide moiety of **7** has the potential to act in metal binding, whereas the carbonyl of the acetyl group on the aromatic ring appears to serve as the surface-recognition area. These interactions contribute to the low inhibition constant for **7**. Compound **10** binds to HDAC8 with two hydrogen bonds (Figure 4B). The hydroxy group at C_{15} of **10** forms the hydrogen bond to ASP101 (2.9 Å), whereas another hydroxy group at C_{14} and the amide group chelate to the zinc ion. The other hydrogen bond occurs between the methoxy group and LYS33 (2.7 Å). The lower *in vitro* inhibitory activity of **10** than that of **7** also correlates well with the calculated binding energy as shown in Table 1. The binding mode of **11** shows no hydrogen bond between the ligand and the enzyme (Figure 4C). However, there is a weak coordination of the methoxy group towards the zinc ion. This weak

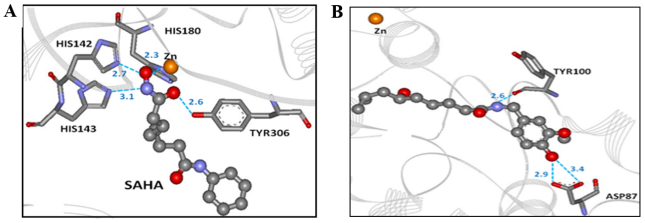

Figure 3. The binding modes of **1** and **6** in the active site of HDAC8.

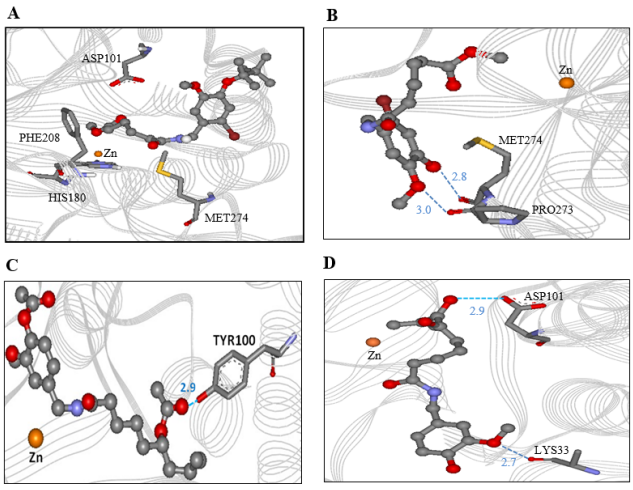

Figure 4. The binding modes of **7**, **10**, **11** and **12** in the active site cavity of HDAC8.

interaction decreases the *in vitro* inhibitory activity of **11** as well. Figure 4D shows the binding mode of **12** in the active site cavity of HDAC, which illustrates that two hydrogen bonds are important for the inhibitor-enzyme binding. The amino group of MET274 (2.8 Å) accepts the hydrogen bond from the phenolic group of **12**. The methoxy group of **12** also binds to the amino group of PRO273 (3.0 Å). The molecular docking results of **13** in the complex with HDAC8 suggest that the *tert*-butyl dimethyl silyl group and the aromatic ring of the ligand are oriented toward the zinc ion (Figure 5). TYR306 makes the close π–π interaction with the phenyl moiety of the ligand. Much of the low free binding energy results from these strong interactions. Analysis of the molecular docking results of compound **13** also revealed that the methoxy and the silyloxy groups in the aromatic region may interact weakly with the zinc ion. Therefore, the phenolic portion of **13** played a critical role for zinc ion binding, not as the surface recognition element. These results correlate with the inhibitory activity of **13** from the *in vitro* experiments.

An independent report from our group showed that **6** possessed a good HDAC inhibitory activity with an IC_{50} value of 72 μM, whereas a commercially available capsaicin acted as only a weak inhibitor (IC_{50} > 13.2 mM) (Senawong *et al.,* 2015). In addition, **6** could also induce apoptosis in HCT116 colon cancer cell lines more efficiently than capsaicin. Toxicity against normal cells of **6** was lower than that of capsaicin as well. The highly potent hydroxamic acids such as TSA were reported to have poor pharmacokinetics and high toxicities (Hahnen *et al.,* 2008; Suzuki *et al.,* 2005). Several non-hydroxamic acids, for instance, curcumin, (*E*)-resveratrol, sinapinic acid and aurones have been developed as HDAC inhibitors to solve these problems (Tatar *et al.,* 2009; Erden *et al.,* 2009; Senawong *et al.,* 2013; Zwick *et al.,* 2014).

4. Conclusions

In conclusion, a series of novel capsaicin and dihydrocapsaicin derivatives were designed and synthesized. All of the previously discussed procedures confirm that capsaicin and dihydrocapsaicin can be utilized as lead compounds for the preparation of various derivatives for biological activity tests. Six derivatives exhibited inhibitory activity against HDAC in the micromolar concentration range. A conventional modification of the phenolic group into a silyl ether resulted in improved activity compared to that of dihydrocapsaicin. Incorporation of hydroxy and dihydroxy groups into the alkyl side chain provided alternative coordination of the zinc ion and resulted in the increased activity. Although their inhibitory activities were not comparable to that of TSA, one compound was already proved to be a potential and safe anticancer agent. The molecular docking studies provided valuable information and allowed us to estimate the free energy of binding, the binding modes, and the inhibition constants. These obtained data show that minor structural changes in capsaicin and dihydrocapsaicin can significantly improve both HDAC inhibitory and anticancer activities.

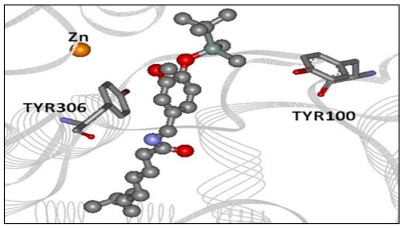

Figure 5. The interaction mode of **13** in the active site of HDAC8.

These novel non-hydroxamic acid HDAC inhibitors should be further studied and developed as anticancer drugs.

Acknowledgements

The Center for Innovation in Chemistry (PERCH-CIC PERDO) and Khon Kaen University are acknowledged for their financial supports of this work. We also would like to thank Assoc. Prof. Dr. Philip J. Proteau for comments and critical review of the manuscript and Mr. Suwatchai Misuna for conducting HDAC assay. A graduate fellowship for Pakit Kumboonma is kindly provided by Rajamangala University of Technology Isan (RMUTI).

References

Bertrand, P. 2010. Inside HDAC with HDAC inhibitors. European Journal of Medicinal Chemistry. 45, 2095-2116.

Cragg, G.M., Grothaus, P.G., and Newman, D.J. 2009. Impact of natural products on developing new anti-cancer agents. Chemical Reviews. 109, 3012-3043.

Erden, D.D., Bora, G., Ayhan, P., Kocaefe, C., Dalkara, S., Yelekci, K., Demir, A.S., and Yurter, H.E. Histone deacetylase inhibition activity and molecular docking of (*E*)-resveratrol: its therapeutic potential in spinal muscular atrophy. 2009. Chemical Biology and Drug Design. 73, 355-364.

Finnin, M.S., Donigian, J.R., Cohen, A., Richon, V.M., Rifkind, R.A., Marks, P.A., Breslow, R., and Pavletich, N.P. 1999. Structures of a histone deacetylase homologue bound to the TSA and SAHA inhibitors. Nature. 401, 188-196.

Hahnen, E., Hauke, J., Trankle, C., Eyupoglu, I.Y., Wirth, B., and Blumcke, I. 2008. Histone deacetylase inhibitors: possible implications for neurodegenerative disorders. Expert Opinion on Investigational Drugs. 17, 169-184.

Hayman, M. and Kam, P.C.A. 2008. Capsaicin: a review of its pharmacology and clinical applications. Current Anesthesia and Critical Care. 19, 338-343.

Kumboonma, P., Phaosiri, C., Misuna, S., Senawong, T., and Yenjai, C. 2009. Isolation and structural modification of capsaicin and dihydrocapsaicin from *Capsicum annuum sp.* Proceedings of the Pure and Applied Chemistry International Conference (PACCON2009), Phitsanulok, Thailand, January 14-16, 2009, 397-400.

Kumboonma, P., Phaosiri, C., Senawong, T., Saiwichai, T., Siriwong, K., and Yenjai, C. 2010. Synthesis and pharmacological evaluation of capsaicin's analogues. Proceedings of the Pure and Applied Chemistry International Conference (PACCON2010), Ubon Ratchathani, Thailand, January 21-23, 2010, 729-732.

Laohavechvanich, P., Kangsadalampai, K., Tirawanchai, N., and Ketterman, A.J. 2006. Effect of different Thai traditional processing of various hot chili peppers on urethane-induced somatic mutation and recombination in *Drosophila melanogaster*: assessment of the role of glutathione transferase activity. Food and Chemical Toxicology. 44, 1348-1354.

Morris, G.M., Huey, R., Lindstrom, W., Sanner, M.F., Belew, R.K., Goodsell, D.S., and Olson, A.J. 2009. AutoDock4 and AutoDockTools4: Automated docking with selective receptor flexibility. Journal of Computational Chemistry. 30, 2785-2791.

Paris, M., Porcelloni, M., Binaschi, M., and Fattori, D. 2008. Histone deacetylase inhibitors: From bench to clinic. Journal of Medicinal Chemistry. 51, 1505-1529.

Sanner, M.F. 1999. Python: A programming language for software integration and development. Journal of Molecular Graphics and Modelling. 17, 57-61.

Senawong, T., Misuna, S., Khaopha, S., Nuchadomrong, S., Sawatsitang, P., Phaosiri, C., Surapaitoon, A., and Sripa, B. Histone deacetylase (HDAC) inhibitory and antiproliferative activities of phenolic-rich extracts derived from the rhizome of *Hydnophytum formicarum* Jack.: sinapinic acid acts as HDAC inhibitor. 2013. BMC Complementary and Alternative Medicine. 13, 232-242.

Senawong, T., Wongphakham, P., Saiwichai, T., Phaosiri, C., and Kumboonma, P. 2015. Histone deacetylase inhibitory activity of hydroxycapsaicin, a synthetic derivative of capsaicin, and its cytotoxic effects against human colon cancer cell lines. Turkish Journal of Biology. 39, 1-10.

Suzuki, T. and Miyata, N. 2005. Non-hydroxamate histone deacetylase inhibitors. Current Medicinal Chemistry. 12, 2867-2880.

Tatar, G.B., Erden, D.D., Demir, A.S., Dalkara, S., Yelekci, K., and Yurter, H.E. Molecular modifications on carboxylic acid derivatives as potent histone deacetylase inhibitors: activity and docking studies. 2009. Bioorganic and Medicinal Chemistry. 17, 5219-5228.

Vannini, A., Volpari, C., Filocamo, G., Casavola, E.C., Brunetti, M., Renzoni, D., Chakravarty, P., Paolini, C., Francesco, R.D., Gallinari, P., Steinkuhler, C., and Marco, S.D. 2004. Crystal structure of a eukaryotic zinc-dependent histone deacetylase, human HDAC8, complexed with a hydroxamic acid inhibitor. Proceedings of the National Academy of Sciences U.S.A. 101, 15064-15069.

Zwick, V., Chatzivasileiou, A.O., Deschamps, N., Roussaki, M., Simoes-Pires, C.A., Nurisso, A., Denis, I., Blanquart, C., Martinet, N., Carrupt, P.A., Detsi, A., and Cuendet, M. Aurones as histone deacetylase inhibitors: Identification of key features. 2014. Bioorganic and Medicinal Chemistry Letters. 24, 5497-5501.